M A N U S C R I P T

for publication in the

International Journal of Hydrogen Energy

Long-term cycle stability of metal hydride-graphite composites

Mila Dieterich[1,*], Carsten Pohlmann[2], Inga Bürger[1], Marc Linder[1] and Lars Röntzsch[2,**]

[1] German Aerospace Center (DLR) - Institute of Engineering Thermodynamics,

Thermal Process Technology, Pfaffenwaldring 38 – 40, 70569 Stuttgart, Germany

[2] Fraunhofer Institute for Manufacturing Technology and Advanced Materials (IFAM),

Branch Lab Dresden, Winterbergstraße 28, 01277 Dresden, Germany

*Corresponding author: phone: +49 (711) 6862-214; fax: +49 (711) 6862-632

    e-mail: Mila.Dieterich@dlr.de

**Corresponding author: phone: +49 (351) 2537-411; fax: +49 (351) 2537-399

    e-mail: Lars.Roentzsch@ifam-dd.fraunhofer.de

Graphical Abstract

Abstract

Recently, metal hydride composites (MHC) have been proposed which consist of a hydride forming metal alloy and a highly heat conduction secondary phase such as expanded natural graphite (ENG) in order to improve the thermal conductivity of metal hydride powder beds. However, only little data is available in the literature on the effects of extensive cycling on technically relevant properties of MHC.

In this paper, hydrogenation characteristics, thermal conductivity and geometrical stability of Hydralloy® C5-based MHC were thoroughly investigated over 1000 cycles. The obtained results suggest that the MHC under study did not significantly alter their hydrogen uptake characteristics throughout cycling, despite the fact that their thermal conductivity decreased during the first 250 cycles but remained constant thereafter. Although the cylindrical MHC maintained their geometrical stability, radial cracks were detected after cycling. Based on these results, MHC are suitable for high-dynamic applications such as hydrogen storage or thermochemical devices.

Keywords

metal hydride; Hydralloy® C5; metal hydride composites (MHC); heat transfer enhancement; cycle stability;

Abbreviations

MHC – metal hydride composite

ENG – expanded natural graphite

Nomenclature

Δp   differential pressure

T   temperature

x   hydrogen uptake

1 Introduction

One of the challenges of renewable energy sources is their volatility. Therefore, energy storage technologies are essential in order to meet the actual energy demand. Surplus electricity, for example, can be stored in form of hydrogen following the electrochemical splitting of water. Hydrogen is a versatile secondary energy carrier that can be used in fuel cells, chemical synthesis or combustion when needed. Metal hydrides are a promising option to store hydrogen at high volumetric density, moderate temperatures and low pressures [1–4].

A specific example where metal hydrides can be used for energy storage refers to domestic applications. Here, hydrogen produced by electrolysis using photovoltaic surplus energy can be stored in a metal hydride. At a later stage, hydrogen is released from the metal hydride storage to feed fuel cells to ensure uninterrupted energy supply [5]. Moreover, the heat of the corresponding exothermal hydride formation (absorption) can be used for thermal applications, for example, heating of domestic water. (See more in [6–8])

For such applications, in addition to a high hydrogen capacity and a high heat of reaction, the metal hydride must also be able to fully absorb and/or desorb hydrogen quickly. Therefore, excellent heat transfer characteristics through the hydride forming material are essential to remove or provide the corresponding heat of reaction. Because metal hydride powders have low intrinsic thermal conductivity [9,10] (in the order of 1 $W \cdot m^{-1} \cdot K^{-1}$ and less), the enhancement of the heat transfer characteristics is necessary. In this regard, plenty of suggestions can be found in the literature [9,11–15]. One of the possible solutions is to mix the hydride forming metal powder with expanded natural graphite (ENG) and fabricate composites from these mixtures. This pathway has been studied for high temperature metal hydrides in recent literature [10,16–18]. Using Hydralloy® C5, a Ti-Mn-base alloy, Pohlmann et al. [19–21] introduced stable compacted metal hydride composites (MHC) with high thermal conductivity for low temperature materials. In this case, the ENG forms a matrix within the MHC, thus, enhancing the thermal conductivity and ensuring sufficient gas permeability at the same time. Furthermore, it is assumed that the percolated ENG network stabilizes the whole MHC

structure. The compaction of hydride forming metal powders with ENG increases the thermal conductivity by more than two orders of magnitude. However, the influence of prolonged cycling on MHC stability, structure and hydrogenation performance has not yet been investigated.

Numerous papers report on the cycle stability of pure metal hydrides [22–28]. For example, Friedlmeier et. al. [29] investigated an AB_2 material ($Ti_{0.98}Zr_{0.02}V_{0.43}Fe_{0.09}Cr_{0.05}Mn_{1.5}$) very similar to Hydralloy® C5 ($Ti_{0.95} Zr_{0.05}Mn_{1.55}V_{0.45}Fe_{0.09}$) used in this paper. Accordingly, no degradation was identified after 42,400 cycles. With regard to the cycle stability of MHC, however, only little data is available [30,31]. Therefore, we have performed intensive experimental studies on the cycling stability of Hydralloy® C5-based MHC with respect to hydrogenation/dehydrogenation performance as well as geometrical stability. Up to 1000 hydrogenation/dehydrogenation cycles were performed using MHC with different ENG contents. In particular, temperature response, hydrogen uptake, thermal conductivity and geometrical stability were investigated. In order to test several MHC in parallel, a specific test rig was designed and brought into operation which allows fully automatic and high-dynamic pressure-induced cycles at constant absorption and desorption pressures.

2   Research setting and methods

2.1. Hydralloy® C5-graphite composites

All MHC under investigation were fabricated using Hydralloy® C5 as hydride-forming metal alloy [19]. Hydralloy® C5 (51 wt.-% Mn, 28 wt.-% Ti, 14 wt.-% V, 3 wt.-% Fe, 3 wt.-% Zr) was purchased from GfE Metalle und Materialien GmbH. The material was delivered in granular form and was milled for 5 min under argon atmosphere. The received Hydralloy® C5 powder was thoroughly mixed with 10 ± 0.1 wt.-% ENG delivered by SGL Carbon. The metal powder-ENG blends were consolidated by uniaxial compaction at 75 MPa into cylindrical MHC with 13.5 mm in diameter and a height of approximately 6.7 mm. Thereafter, a 2 mm central hole was drilled to ensure fast gas transport in axial direction. The according residual porosity within the samples was calculated on the basis of the theoretical

density of each MHC using the theoretical density of ENG of about 2.1 g·cm^{-3} and Hydralloy® C5 of about 6.1 g·cm^{-3} [19]. The radial effective thermal conductivities of selected MHC samples were examined before and after cycling via the nano flash method applying a gas tight measuring cell. The complete processing chain and analytic details are described in a previous work [32].

2.2. Test rig

2.2.1. Test rig layout

To investigate the long-term cycle stability of MHC, a special test rig was developed and brought into operation. It enables us to control and monitor large quantities of up to the kilogram range of reaction material for extensive number of cycles which allows the investigation of complete structures, e.g. matrixes for heat transfer enhancement in metal hydride composites. Four parallel test reactors with MHC samples can be monitored regarding their hydrogenation performance, MHC sample temperature and gas uptake dynamics at the same time. In particular, the time-dependence of these values during cycling is of interest. The test rig can be operated automatized at temperature levels between 50 °C and 400 °C and at hydrogen pressures up to 100 bar. During cycling large temperature changes inside the MHC occur which are tempered using a thermal fluid connected to a thermostatic bath at constant temperature. The hydrogen gas pressure can be increased or decreased quickly (in the order of seconds), thus, high-dynamic hydrogenation-dehydrogenation tests can be conducted. A schematic layout of the test rig is depicted in Figure 1.

The temperature development within each MHC sample is monitored using a 1 mm thermocouple of type K. The thermocouple is positioned in the middle of the MHC, as here the highest temperature gradient is expected. Furthermore, the temperature within the heat transfer fluid is measured at several positions with PT100 temperature sensors. The flow rate of the heat transfer fluid is set as high as to guarantee a constant and almost identical (± 1 K) temperature for all reactors. The hydrogen pressure inside the reactors is monitored using a pressure sensor (measuring accuracy:

uncertainty of measurement of ±0.6 bar, reproducibility of ±0.12 bar). The overall hydrogen uptake is measured by an included Sievert's apparatus, as explained in the following.

2.2.2. Determining the hydrogen uptake by Sieverts' method

The Sieverts' method is used here to determine the hydrogen uptake of the MHC and, more importantly, to determine any changes in the hydrogen uptake as a function of the cycle number. The method is also referred to as volumetry or manometry [33]. In general, the Sieverts' apparatus consists of a known volume (here called Sieverts' volume including all tubing, $V_{Sieverts'}$) filled with hydrogen and a pressure sensor. The measured pressure drop is directly correlated to the mass of hydrogen leaving the Sieverts' volume. In the present configuration, the Sieverts´ volume and the volume of the four test reactors are separated by a control valve. Therefore, the pressure in the reactors can be controlled at a set point, which is kept constant throughout absorption independent of the amount of absorbed hydrogen and of the pressure in the Sieverts' volume. The absorption pressure can be set between 1 bar and 100 bar.

All instruments used in the present setup are calibrated by the manufacturers. Data transmission errors are corrected. For the present set-up with pressures up to 70 bar, the error in mass due to the compressibility of hydrogen (3.4% at 25°C [34]) is neglected. A detailed guideline for an accurate measurement is given in Broom et al. [28]. However, since the aim of these measurements is neither the determination of thermodynamic or kinetic properties of the pure material nor the operation below atmospheric pressure the aspects that need to be considered are reduced to the following two points: Accuracy of pressure measurement and free volume correction.

Accuracy of pressure measurement

To realize a high accuracy of the pressure measurement even at high absorption pressures, a differential pressure sensor (ΔP) and a small reference volume are added to the apparatus (cf. Figure 1). By separating this volume at initial pressure, the pressure change in the Sieverts' volume is

measured during the experiments. Thereby, a high accuracy of 0.05 bar for pressure differences up to 10 bar can be achieved. The measurement range of the used pressure sensor enables the measurement of a wide range of materials with different hydrogen storage capacities and densities. Thus, it also allows a sufficient accuracy for the measurements, especially with a focus on cycling stability. For higher pressure differences, the pressure of the Sieverts' volume is measured directly by an absolute-pressure sensor (P2) with an accuracy of 0.8 bar up to 100 bar. For the measurements in this study, the sample size was chosen to cause a pressure difference of less than 10 bar in the Sieverts' volume to gain high accuracy.

Free volume correction

For absorption, the volume of the tubing, reactors, and porosity of the material is filled with hydrogen which is not absorbed but causes a pressure drop in the Sieverts' volume. Therefore, a correction of this free volume is needed as described by Rouquerol in [35].

The free volume varies during cycling due to the volume changes of the metal hydride during absorption and desorption. The calculation of the volume-mass relationship given by Wang and Suda [36] showed that the system volume is big enough compared to the MHC mass and, therefore, the volume change of material during cycling and, thus, the change of the free volume is insignificant.

The free volume was measured at low pressures, where hydrogen is assumed to behave as an ideal gas. The duration of measurement was long enough for all temperatures to return to their initial values. For the measurement, absorption has to be excluded. This can be achieved, depending on the material, either by measuring at a different temperature, with an inert gas, before activation or without the material. The transfer to the experiment for the first two options can be calculated with the ideal gas law including reality factors if necessary. If measuring without material its volume calculated from its mass and density has to be considered (see Appendix). Because Hydralloy® C5 is very reactive, we chose to measure without material. From the ideal gas law, the pressure drop with material can be calculated. See the Appendix for more detail.

Calculation of hydrogen uptake

The mass of hydrogen absorbed can then be determined with the ideal gas law. Knowing the mass of the metal hydride in the MHC, the hydrogen uptake can be calculated.

Concluding this section, it has to be noted that the determined reversible hydrogen uptake is subject to errors, as mentioned before. However, the intention of the present setup is the investigation of changes in this value as a function of the number of cycles. As the reproducibility of all values is very high, such changes can be determined accurately and, therefore, give important information about possible degradation of the MHCs.

2.2.3. Test reactors

Four equally sized cylindrical test reactors made from stainless steel with an inner diameter of 13.5 mm were placed in containers connected with the thermostatic bath. Each of the test reactors was filled with four MHC bodies (pellets) with a total height of about 27 mm (height-diameter-ratio of 2:1) in-between two cylindrical pieces of teflon (each with a height of 13.5 mm) to ensure thermal insulation in axial direction (cf. Figure 2). The thermal insulation in axial direction was included in order to be able to focus mainly on the thermal conductivity of the MHC in radial direction. It can be excluded that teflon chemically interferes with the hydrogen uptake of the MHC under study. The axial position of the thermocouple within the MHC was set to approximately half of the total MHC height.

2.2.4. Testing procedure

The MHC samples were activated and cycled with hydrogen of 99.999 % purity. First, the MHC were activated by applying two cycles of 2 h at 130 °C and hydrogen pressure at 5 bar and vacuum, respectively, and one cycle at 50 °C and hydrogen pressure at 30 bar for 13 h and vacuum for half an

hour, respectively. Then, the MHCs were cycled at a constant temperature of 50 °C. The absorption pressure was set to 40 bar and desorption pressure to 1 bar. Both absorption and desorption took place very quickly (in the order of 2 to 5 min) leading to a significant change in MHC temperature. A change in this peak temperature during cycling has been used as one indication for a change in thermal conductivity.

2.3. MHC geometrical stability after cycling

After cycling, the reactors were opened under inert atmosphere in order to extract the MHC. A 3 mm Swagelok connector at the bottom of the reactors (cf. Figure 2) can be opened to push the MHC. However, due to a slight volume swelling of the MHC due to cycling, an intimate contact between the MHC and the inner reactor walls was observed which increased wall friction drastically. Therefore, in many cases the MHC were damaged during removal (fractures, deformations and break-offs of the MHC). Thus, only a qualitative impression of the geometrical stability can be given.

3   Results and discussion

In the present paper, the hydrogenation properties and geometrical stability of Hydralloy® C5-based MHC were investigated. For this purpose, identical MHC with an ENG-content of 10 wt.-% and a residual porosity of approx. 30 % were fabricated. At first, a cycling time of 10 minutes (5 min absorption + 5 min desorption) was applied for 1000 cycles. The hydrogenation/dehydrogenation performance was observed throughout cycling, whereas the mechanical stability and thermal conductivity were determined after 250, 500, 750, and 1000 cycles by stepwise removing the MHC bodies (pellets) from the four identical reactors.

The applied cycling time of only 10 minutes seemed to have an influence on the development of hydrogen uptake. Therefore, another identical MHC was cycled with a longer cycling time of 60 minutes (30 min absorption + 30 min desorption) for only 100 cycles. Again, hydrogenation performance and mechanical stability after 100 cycles were determined.

3.1. Cycling stability of hydrogenation performance

The relative amounts of absorbed hydrogen (hydrogen uptake) of MHC are presented in Figure 3. To compare the four samples, their hydrogen capacity was normalized to the maximum hydrogen capacity of sample MHC-D after 1000 cycles which corresponds to approximately 1.5 wt.-%. Furthermore, the maximum temperatures of the MHC samples during absorption ($T_{peak,abs}$) and the minimum temperatures during desorption ($T_{peak,des}$) are plotted. From these curves, the following conclusions can be drawn:

First, it can be seen that the hydrogen capacity after 5 min of absorption (hydrogen uptake) increases with increasing cycle number starting from about 70 % of the nominal capacity. All MHC samples follow the same trend. After 600 cycles, the full hydrogen capacity is reached. The hydrogen uptake never declines compared to the prior cycle (see absolute values in Figure 3) except for cycle 550. Before this cycle, the test bench had to be modified and the MHCs were stored at room temperature in hydrogen at desorption pressure for four weeks. The effect is clearly visible as a decrease in

hydrogen uptake compared to before. Thus, in view of hydrogen uptake, the prepared MHC exhibit a stable cycling behavior over 1000 cycles.

Second, the peak temperatures of all MHC samples are on the same quantitative level throughout all cycles. According to Figure 3, a slight deviation is observed for sample MHC-B where the peak temperatures are about 10 K closer to the temperature of the thermostatic bath for the first 120 cycles. Afterwards, the temperature signals are very similar to the other MHC samples. This deviation might be caused by slight sample displacements relative to the thermocouple due to sample transport. Nevertheless, regarding the peak temperatures during absorption and desorption, it is legitimate to state that the MHC exhibit a stable hydrogenation performance over 1000 cycles.

In order to discuss the cycle-dependent hydrogen uptake dynamics of MHC in more detail, Figure 4 presents the temperature development at the center of the MHC (straight lines) and the corrected differential hydrogen pressure development (dashed lines) after the 25th, 50th, 250th, 500th, 750th, and 1000th cycle. Furthermore, an inset provides the total hydrogen uptake after the respective cycle.

The curves of the differential pressure show a very steep increase within the first 20 s of a cycle; afterwards a slight decrease is recognizable before the curves increase again to their maximum values. The slight decrease might be explained by artefacts of the pressure measurement, which occur when the rapidly flowing hydrogen vigorously pulls at the membrane of the pressure sensor. Therefore, the differential pressure curve does not represent the precise course of the hydrogen uptake. Thus, only the maximum values of hydrogen uptake for each cycle are given. The results illustrate the steady increase in hydrogen capacity up to 1.54 wt.-% for the 1000th cycle.

Figure 4 also demonstrates that the temperature profiles of the MHC are nearly equal for all cycles. As the hydrogen uptake of Hydralloy C5 is very sensible to temperature [37], the increase in temperature during absorption limits the hydrogen uptake. Therefore, during cooling more hydrogen can be absorbed and heat is released leading to a slower decline of the temperature. As soon as the hydrogenation reaction is almost finished, the temperature decreases faster. This rapid cooling can

be clearly detected in Figure 4 after approximately 1.5 min (grey dotted line). From this point onward, the differential pressure still exhibits a very slight increases which can be explained by the PCT characteristics of Hydralloy® C5, whose plateau length grows with decreasing temperature [37].

Summarizing the results presented in Figure 3 and Figure 4 it can be stated that the amount of hydrogen absorbed within 5 min increases starting from 70 % to 100 % of the nominal capacity till the 600th cycle is reached and stays constant thereafter throughout the 1000th cycle. Furthermore, the peak temperature of all MHCs is constant, and the temperature development at the center of the MHC is nearly equal for all cycles. Thus, these results provide evidence concerning the stability of hydrogenation performance of the investigated Hydralloy C5-based MHC for 1000 cycles. Additionally, it can be stated that the MHC under investigation can absorb more than 90 % of the nominal hydrogen capacity within 1.5 min throughout the whole cycling test, which underlines their applicability in high dynamic operation modes.

3.2. Thermal conductivity and geometrical stability

The radial thermal conductivity of the MHCs after the 250th, 500th, 750th, and 1000th cycle is given in Figure 5. The thermal conductivity decreases from about 40 $W·m^{-1}·K^{-1}$ for the uncycled MHC to 12.7 $W·m^{-1}·K^{-1}$ after 250 cycles. From our previous work [32] we deduce that the drop in thermal conductivity occurs within the first few cycles (< 20). This value is stabilizing in a range of about 10 to 15 $W·m^{-1}·K^{-1}$ for all cycles thereafter. Thus, the thermal conductivity of cycled MHCs is still significantly higher than that of commonly used loose powder beds. This is also evident in the response of MHC-D (see Figure 4). Consequently, a constant technical performance of a hydrogen storage device based on MHC can be expected.

Furthermore, the geometrical integrity of the MHC is maintained throughout cycling. Figure 6 depicts two pellets of sample MHC-D after 1000 cycles in comparison with their as-compacted state. It is obvious that the MHC still preserve their original cylindrical shape including the central hole. Nonetheless, their height is slightly increased and various radial cracks are observed.

However, a strong stability within the radial planes can be deduced. Thus, the fast radial heat transfer is preserved which can be seen in the measured thermal conductivities as well as in the hydrogenation performance that allowed fast cycling throughout all 1000 cycles.

In this case, the MHC were not constrained regarding their axial expansion during cycling. If they had been axially confined, an even more stable and more dynamic MHC would have resulted. However, additional mechanical forces acting upon the tank wall, which are attributed to the MHC volume swelling, would have evolved during hydrogen uptake.

3.3. Extension of cycling time

As mentioned in Section 3.1, the duration of hydrogen absorption seemed to have an influence on the activation of the materials: When cycled at short cycle times of 10 min, the amount of hydrogen uptake increases for approximately 600 cycles before it remained constant thereafter. In order to test whether a longer cycling time would reduce the number of cycles before the maximum hydrogen uptake is reached, one MHC was cycled over 60 min (30 min absorption + 30 min desorption), the results of which are presented in Figure 7. Similarly to the short cycle time an increase in hydrogen uptake is noticeable, however, on a higher relative level. Already after the 93rd cycle the amount of hydrogen uptake equals that of the 1000th cycle when a short cycling time was applied (cf. Figure 4). In both cases, the total absorption time adds up to the same value of 3000 min: 600 cycles with 5 min absorption and 100 cycles with 30 min absorption. Therefore, it is obvious that absorption time has an influence on hydrogen uptake, however, it is not completely clear which one is the main effect: the absorption time per cycle or the total absorption time.

4   Conclusion

This paper reports on the hydrogenation performance, thermal conductivity and the mechanical stability of Hydralloy® C5-based MHCs with an ENG-content of 10 wt.-% throughout 1000 cycles. The MHC showed constant temperature responses and increasing or constant hydrogen uptake throughout all 1000 cycles. The thermal conductivity decreased after the first 250 cycles but was constant afterwards in a range of about 10 to 15 $W \cdot m^{-1} \cdot K^{-1}$. Furthermore, after removing the MHC from the reactors they still showed high geometrical stability, both of which leads to stable and highly dynamic loading and unloading performance with a hydrogen uptake time of about 1.5 minutes. Additionally, the influence of the cycle time on the activation process was demonstrated.

Based on these results, Hydralloy® C5-based MHC can be considered suitable for various technical applications.

References

[1]   Sandrock G, Suda S, Schlapbach L. Applications. In: Schlapbach L, editor. Hydrog. Intermet. Comounds II - Surf. Dyn. Prop. Appl., Springer-Verlag; 1992, p. 197–258. doi:10.1007/3-540-54668-5.

[2]   Botzung M, Chaudourne S, Gillia O, Perret C, Latroche M, Percheron-Guegan A, et al. Simulation and experimental validation of a hydrogen storage tank with metal hydrides. Int J Hydrogen Energy 2008;33:98–104. doi:10.1016/j.ijhydene.2007.08.030.

[3]   Züttel A. Hydrogen storage methods. Naturwissenschaften 2004;91:157–72. doi:10.1007/s00114-004-0516-x.

[4]   Utz I, Linder M, Schmidt N, Hu JJ, Fichtner M, Wörner A. Experimental study of powder bed behavior of sodium alanate in a lab-scale H2 storage tank with flow-through mode. Int J Hydrogen Energy 2012;37:7645–53. doi:10.1016/j.ijhydene.2012.02.016.

[5]   Maeda T, Fuura T, Matsumoto I, Kawakami Y, Masuda M. Cyclic stability test of AB2 type (Ti, Zr)(Ni, Mn, V, Fe)2.18 for stationary hydrogen storage in water contaminated hydrogen. J Alloys Compd 2013;580:S255–8. doi:10.1016/j.jallcom.2013.03.230.

[6]   Young K, Hills R. Metal Hydrides. Elsevier Inc.; 2013. doi:10.1016/B978-0-12-409547-2.05894-7.

[7]   Bhuiya MMH, Kumar A, Kim KJ. Metal hydrides in engineering systems, processes, and devices: A review of non-storage applications. Int J Hydrogen Energy 2015. doi:10.1016/j.ijhydene.2014.12.009.

[8]   Muthukumar P, Groll M. Metal hydride based heating and cooling systems: A review. Int J Hydrogen Energy 2010;35:3817–31. doi:10.1016/j.ijhydene.2010.01.115.

[9]   Kim KJ, Montoya B, Razani A, Lee K-H. Metal hydride compacts of improved thermal conductivity. Int J Hydrogen Energy 2001;26:609–13. doi:10.1016/S0360-3199(00)00115-4.

[10]   Chaise a., de Rango P, Marty P, Fruchart D. Experimental and numerical study of a magnesium hydride tank. Int J Hydrogen Energy 2010;35:6311–22. doi:10.1016/j.ijhydene.2010.03.057.

[11]   Anbarasu S, Muthukumar P, Mishra SC. Tests on LmNi4.91Sn0.15 based solid state hydrogen storage device with embedded cooling tubes – Part A: Absorption process. Int J Hydrogen Energy 2014. doi:10.1016/j.ijhydene.2013.12.090.

[12]   Meng X, Wu Z, Bao Z, Yang F, Zhang Z. Performance simulation and experimental confirmation of a mini-channel metal hydrides reactor. Int J Hydrogen Energy 2013;1–12. doi:10.1016/j.ijhydene.2013.09.056.

[13]   Dehouche Z, de Jong W, Willers E, Isselhorst A, Groll M. Modelling and simulation of heating/air-conditioning systems using the multi-hydride-thermal-wave concept. Appl Therm Eng 1998;18:457–80. doi:10.1016/S1359-4311(97)00043-4.

[14]   Rodríguez Sánchez A, Klein H-P, Groll M. Expanded graphite as heat transfer matrix in metal hydride beds. Int J Hydrogen Energy 2003;28:515–27. doi:10.1016/S0360-3199(02)00057-5.

[15]   Kim J-H, Kim J-H, Hwang K-T, Kang Y-M. Hydrogen storage in magnesium based-composite hydride through hydriding combustion synthesis. Int J Hydrogen Energy 2010;35:9641–5. doi:10.1016/j.ijhydene.2010.06.099.

[16]   Jehan M, Fruchart D. McPhy-Energy's proposal for solid state hydrogen storage materials and systems. J Alloys Compd 2013;580:S343–8. doi:10.1016/j.jallcom.2013.03.266.

[17]   Chaise a., de Rango P, Marty P, Fruchart D, Miraglia S, Olivès R, et al. Enhancement of hydrogen sorption in magnesium hydride using expanded natural graphite. Int J Hydrogen Energy 2009;34:8589–96. doi:10.1016/j.ijhydene.2009.07.112.

[18]   Van Hassel B a., Mosher D, Pasini JM, Gorbounov M, Holowczak J, Tang X, et al. Engineering improvement of NaAlH4 system. Int J Hydrogen Energy 2012;37:2756–66. doi:10.1016/j.ijhydene.2011.02.005.

[19]   Pohlmann C, Röntzsch L, Weißgärber T, Kieback B. Heat and gas transport properties in pelletized hydride–graphite-composites for hydrogen storage applications. Int J Hydrogen Energy 2013;38:1685–91. doi:10.1016/j.ijhydene.2012.09.159.

[20]   Heubner F, Pohlmann C, Mauermann S, Kieback B, Röntzsch L. Mechanical stresses originating from metal hydride composites during cyclic hydrogenation. Int J Hydrogen Energy 2015;40:10123–30. doi:10.1016/j.ijhydene.2015.06.053.

[21]   Herbrig K, Pohlmann C, Gondek Ł, Figiel H, Kardjilov N, Hilger A, et al. Investigations of the structural stability of metal hydride composites by in-situ neutron imaging. J Power Sources 2015;293:109–18. doi:10.1016/j.jpowsour.2015.05.039.

[22]   Wanner M, Friedlmeier G, Hoffmann G, Groll M. Thermodynamic and structural changes of various intermetallic compounds during extended cycling in closed systems. J Alloys Compd 1997;253-254:692–7. doi:10.1016/S0925-8388(96)03041-1.

[23]   Lambert SW, Chandra D, Cathey WN, Lynch FE, Bowman RC. Investigation of hydriding properties of LaNi4.8Sn0.2, LaNi4.27Sn0.24 and La0.9Gd0.1Ni5 after thermal cycling and aging. J Alloys Compd 1992;187:113–35. doi:10.1016/0925-8388(92)90527-G.

[24]   Bowman RC, Luo CH, Ahn CC, Witham CK, Fultz B. The effect of tin on the degradation of LaNi5−ySny metal hydrides during thermal cycling. J Alloys Compd 1995;217:185–92. doi:10.1016/0925-8388(94)01337-3.

[25]   Bershadsky E, Josephy Y, Ron M. Investigation of kinetics and structural changes in TiFe0.8 Ni0.2 after prolonged cycling. J Less Common Met 1991;172-174:1036–43. doi:10.1016/S0022-5088(06)80009-3.

[26]   Dehouche Z, Djaozandry R, Huot J, Boily S, Goyette J, Bose T., et al. Influence of cycling on the thermodynamic and structure properties of nanocrystalline magnesium based hydride. J Alloys Compd 2000;305:264–71. doi:10.1016/S0925-8388(00)00718-0.

[27]   Lototskyy MV, Yartys VA, Pollet BG, Bowman RC. Metal hydride hydrogen compressors: A review. Int J Hydrogen Energy 2014;39:5818–51. doi:10.1016/j.ijhydene.2014.01.158.

[28]   Josephy Y, Bershadsky E, Ron M. Investigation of LaNi5 after prolonged cycling. J Less Common Met 1991;172-174:997–1008. doi:10.1016/S0022-5088(06)80005-6.

[29] Friedlmeier G, Manthey A, Wanner M, Groll M. Cyclic stability of various application-relevant metal hydrides. J Alloys Compd 1995;231:880–7. doi:10.1016/0925-8388(95)01776-3.

[30] Josephy Y, Eisenberg Y, Perez S, Ben-David A, Ron M. Hydrogen and thermal yields of porous metal matrix hydride compacts of MmNi4.15Fe0.85Hx. J Less Common Met 1984;104:297–305. doi:10.1016/0022-5088(84)90414-4.

[31] Ron M, Bershadsky E, Joseph Y. Thermal conductivity of PMH compacts, measurements and evaluation. Int J Hydrogen Energy 1992;17:623–30. doi:10.1016/0360-3199(92)90076-9.

[32] Pohlmann C, Röntzsch L, Heubner F, Weißgärber T, Kieback B. Solid-state hydrogen storage in Hydralloy–graphite composites. J Power Sources 2013;231:97–105. doi:10.1016/j.jpowsour.2012.12.044.

[33] Broom D. The accuracy of hydrogen sorption measurements on potential storage materials. Int J Hydrogen Energy 2007;32:4871–88. doi:10.1016/j.ijhydene.2007.07.056.

[34] US Department of Commerce N. National Institute of Standards and Technology n.d. http://www.nist.gov/ (accessed August 13, 2015).

[35] Rouquerol F, Rouquerol J, Sing K. Adsorption by Powders and Porous Solids. Elsevier; 1999. doi:10.1016/B978-012598920-6/50004-X.

[36] Wang X-L, Suda S. Consistent determination of the intrinsic kinetic properties between hydrogen and hydriding alloys. J Alloys Compd 1995;231:660–5. doi:10.1016/0925-8388(95)01748-8.

[37] Herbrig K, Röntzsch L, Pohlmann C, Weißgärber T, Kieback B. Hydrogen storage systems based on hydride–graphite composites: computer simulation and experimental validation. Int J Hydrogen Energy 2013;38:7026–36. doi:10.1016/j.ijhydene.2013.03.104.

List of figures

Figure 1: Schematic layout of the test rig with four test reactors and a Sievert's volume.

Figure 2: Stainless steel test reactor for cyclic hydrogenation of MHC

Figure 3: Normalized hydrogen uptake and peak temperatures of MHC at a cycle time of 10 min (5 min absorption + 5 min desorption).

Figure 4: Temperature T, corrected differential pressure Δp and hydrogen uptake x

Figure 5: Development of the radial thermal conductivity of MHC throughout 1000 cycles.

Figure 6: Sample MHC-D before (small picture) and after (large picture) 1000 cycles.

Figure 7: Corrected differential pressure and hydrogen uptake of a MHC for a cycle time of 60 minutes.

Appendix: Details to free volume correction

The free volume V_{free} is calculated by $V_{free} = \frac{\Delta p_{Sieverts'} V_{Sieverts'} T_{reactor}}{\Delta p_{reactor} T_{Sieverts'}} - V_{MHC}$, where $\Delta p_{Sieverts'}$

is the pressure drop in the Sieverts' volume due to absorption, $\Delta p_{reactor}$ is the pressure increase in

the reactor, $T_{Sieverts'}$ and $T_{reactor}$ are the absolute temperatures in the Sieverts' volume and the

reactor, respectively, and V_{MHC} is the volume of the MHC. The latter is calculated from the mass and

density of the material. For the present setup, the biggest influence on the accuracy of the free

volume has been by far the measurement of the pressure differences. This is because of the small

changes in pressure when no reaction takes place, hence, the difference of the measured values is

close to the value of accuracy.

The pressure drop in the Sieverts' volume caused by the free space $\Delta p_{Sieverts' free}$ can be calculated

for cycling conditions by $\Delta p_{Sieverts' free} = \frac{\Delta p_{reactor} V_{free} T_{Sieverts'}}{T_{reactor} V_{Sieverts'}}$. Here, the determination of the

free volume has the biggest influence on the accuracy.
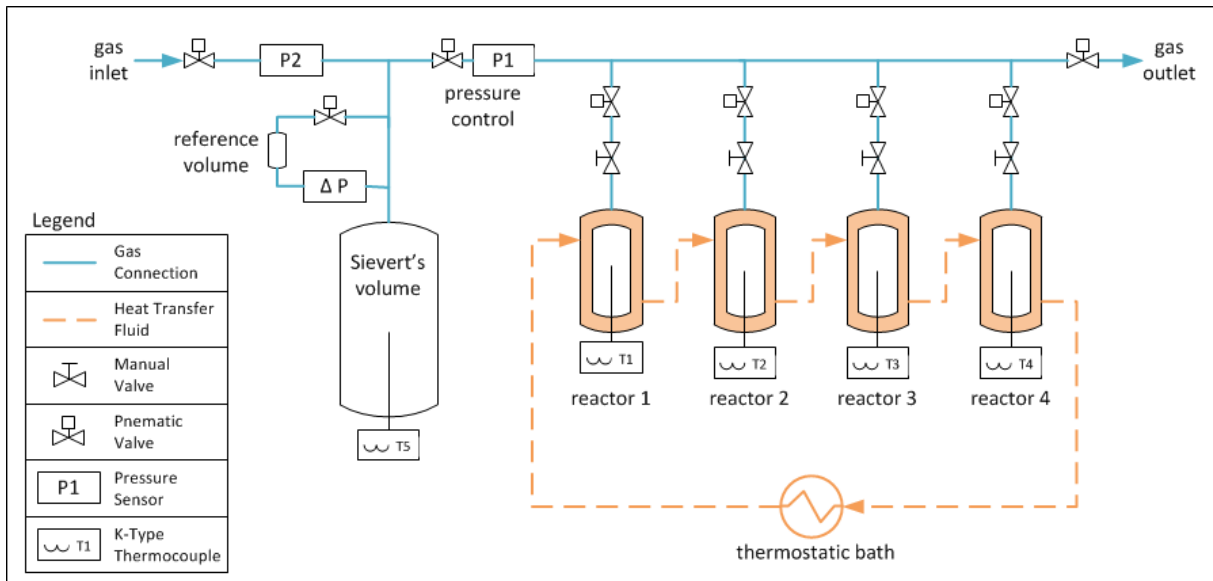
Figures
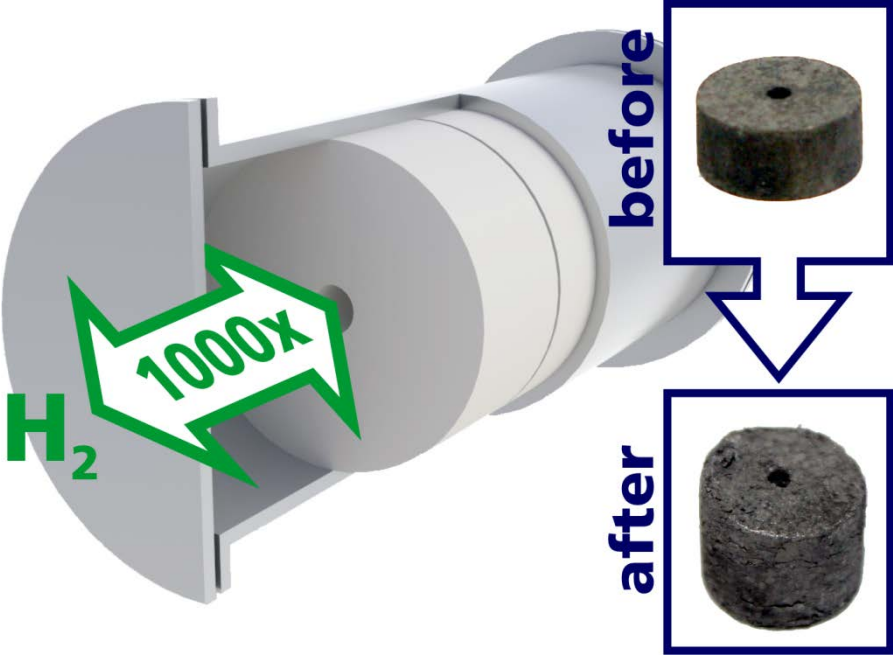
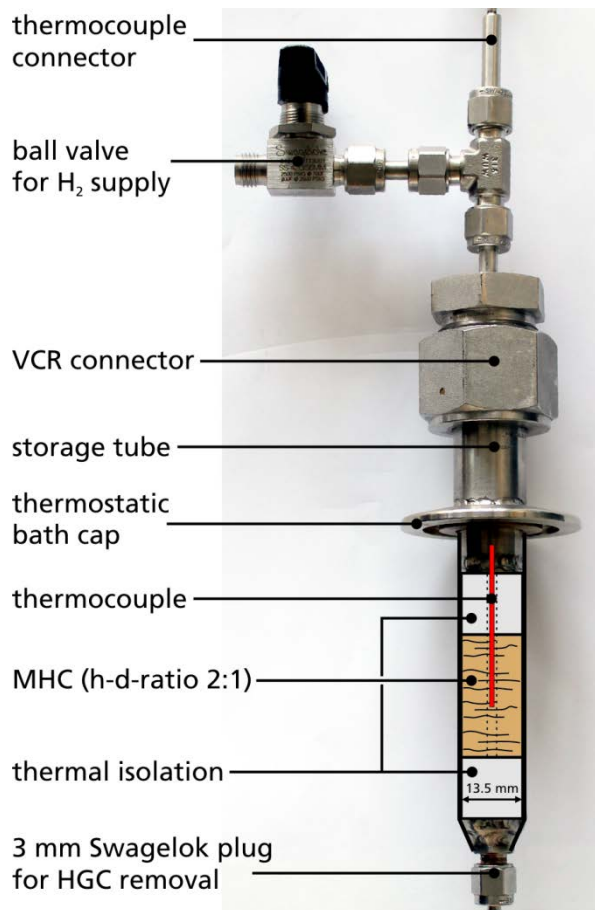Graphical Abstract

Fig1 Schematic layout of the test rig

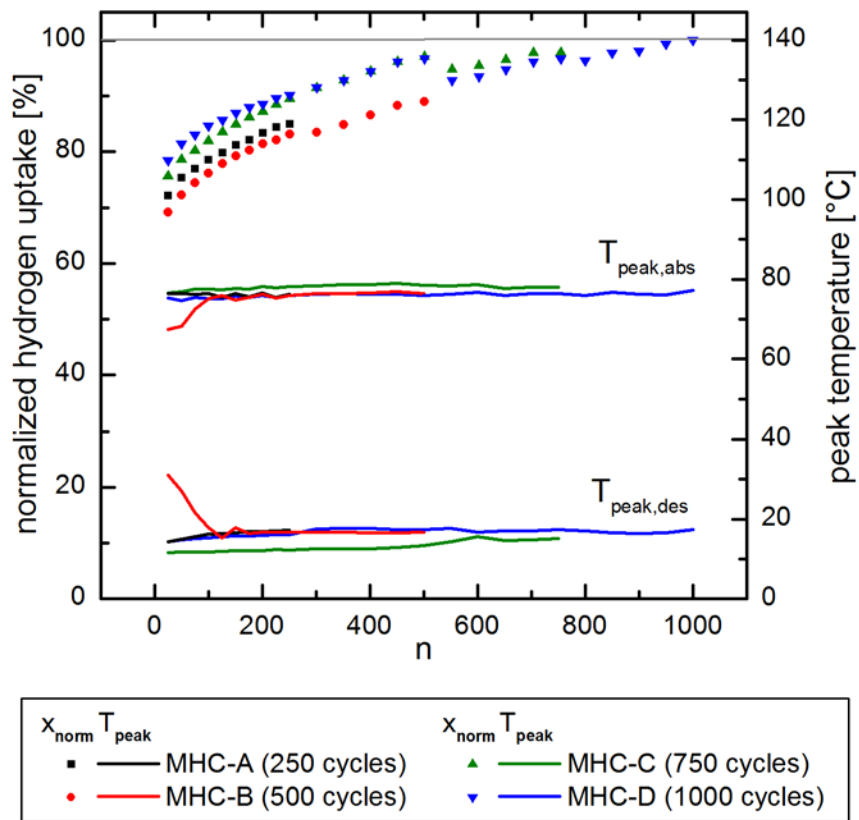Fig2 Stainless steel test reactor for cyclic hydrogenation of MHC

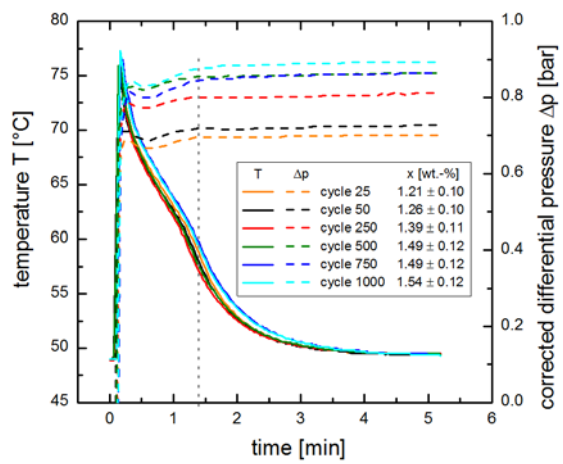Fig3 Normalized hydrogen uptake and peak temperatures of MHC

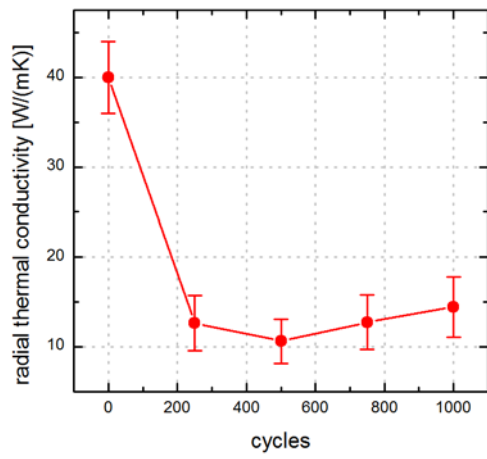Fig4 Temperature T, corrected differential pressure Δp

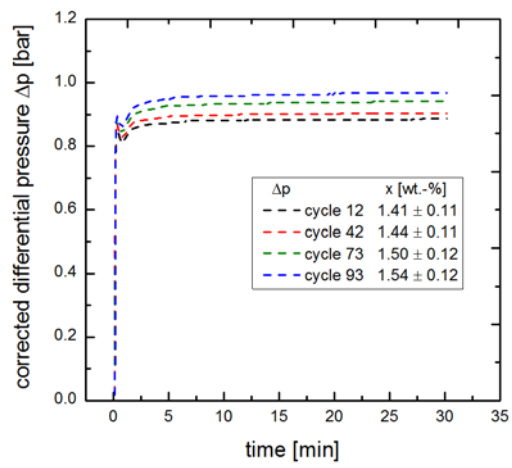Fig5 Development of the radial thermal conductivity of MHC

Fig6 Sample MHC-D before and after 1000 cycles

Fig7 Corrected differential pressure and hydrogen uptake